

1 **A potential cortical precursor of visual word form recognition in untrained monkeys**

2 *Rishi Rajalingham*<sup>1,2</sup>, *Kohitij Kar*<sup>1,2,3</sup>, *Sachi Sanghavi*<sup>1,2</sup>, *Stanislas Dehaene*<sup>4,5</sup>, *James J. DiCarlo*<sup>1,2,3</sup>

3

4 <sup>1</sup>Department of Brain and Cognitive Sciences, <sup>2</sup>McGovern Institute for Brain Research, <sup>3</sup>Center for Brains, Minds  
5 and Machines

6 Massachusetts Institute of Technology, Cambridge, Massachusetts 02139

7 <sup>4</sup>Collège de France, 11 Place Marcelin Berthelot, 75005 Paris, France

8 <sup>5</sup>Cognitive Neuroimaging Unit, CEA, INSERM, Université Paris-Sud, Université Paris-Saclay, NeuroSpin center,  
9 91191 Gif/Yvette, France

10

11 Correspondence should be addressed to James J. DiCarlo, McGovern Institute for Brain Research, Department of  
12 Brain and Cognitive Sciences, Massachusetts Institute of Technology, 77 Massachusetts Institute of Technology,  
13 46-6161, Cambridge, MA 02139. E-mail: [dicarlo@mit.edu](mailto:dicarlo@mit.edu)

14

15 *Title: 12 words*

16 *Abstract: 321 words*

17 *Introduction: 995 words*

18 *Discussion: 1308 words*

19 *Figures: 4*

20

21 **Abstract**

22

23 Skilled human readers can readily recognize written letters and letter strings. This domain of visual recognition,  
24 known as orthographic processing, is foundational to human reading, but it is unclear how it is supported by neural  
25 populations in the human brain. Behavioral research has shown that non-human primates (baboons) can learn to  
26 distinguish written English words from pseudo-words (lexical decision), successfully generalize that behavior to novel  
27 strings, and exhibit behavioral error patterns that are consistent with humans. Thus, non-human primate models,  
28 while not capturing the entirety of human reading abilities, may provide a unique opportunity to investigate the  
29 neuronal mechanisms underlying orthographic processing. Here, we investigated the neuronal representation of  
30 letters and letter strings in the ventral visual stream of naive macaque monkeys, and asked to what extent these  
31 representations could support visual word recognition. We recorded the activity of hundreds of neurons at the top  
32 two levels of the ventral visual form processing pathway (V4 and IT) while monkeys passively viewed images of  
33 letters, English words, and non-word letter strings. Linear decoders were used to probe whether those neural  
34 responses could support a battery of orthographic processing tasks such as invariant letter identification and lexical  
35 decision. We found that IT-based decoders achieved baboon-level performance on these tasks, with a pattern of  
36 errors highly correlated to the previously reported primate behavior. This capacity to support orthographic processing  
37 tasks was also present in the high-layer units of state-of-the-art artificial neural network models of the ventral stream,  
38 but not in the low-layer representations of those models. Taken together, these results show that the IT cortex of  
39 untrained monkeys contains a reservoir of precursor features from which downstream brain regions could, with some  
40 supervised instruction, learn to support the visual recognition of written words. This suggests that the acquisition of  
41 reading in humans did not require a full rebuild of visual processing, but rather the recycling of a brain network  
42 evolved for other visual functions.

43

## 44 Introduction

45

46           Literate human adults can efficiently recognize written letters and their combinations over a broad range of  
47 fonts, scripts and sizes (1–3). This domain of visual recognition, known as orthographic processing, is foundational  
48 to human reading abilities, because the invariant recognition of the visual word form is an indispensable step prior  
49 to accessing the sounds (phonology) and meanings (semantics) of written words (4). It is largely unknown how  
50 orthographic processing is supported by neural populations in the human brain. Given the recency of reading and  
51 writing to the human species (a cultural invention dating to within a few thousand years), it is widely believed that the  
52 human brain could not have evolved *de novo* neural mechanisms for the visual processing of orthographic stimuli,  
53 and that the neural representations that underlie orthographic processing abilities must build upon, and thus be  
54 strongly constrained by, the prior evolution of the primate brain (5, 6). In particular, a dominant theory is that the  
55 ventral visual pathway, a hierarchy of cortical regions known to support visual object recognition behaviors, could be  
56 inherited from recent evolutionary ancestors and minimally repurposed (or “recycled”) through developmental  
57 experience to support orthographic processing (6). Consistent with this hypothesis, functional imaging studies  
58 suggest that the post-natal acquisition of reading is accompanied by a partial specialization of dedicated cortical sub-  
59 regions in the human ventral visual pathway, which ultimately become strongly selective to orthographic stimuli (7–  
60 9). However, given the limitations of human imaging methods, it has been challenging to quantitatively test if and  
61 how neural representations in the ventral visual pathway might be reused to support orthographic processing.

62

63           Interestingly, the ventral visual processing stream – a hierarchically-connected set of neocortical areas (10)  
64 – appears remarkably well conserved across many primate species, including Old World monkeys, such as a rhesus  
65 macaques (*Macaca mulatta*) and baboons (*Papio papio*), that diverged from humans about 25 million years ago (11).  
66 Indeed, decades of research have inferred strong anatomical and functional homologies of the ventral visual  
67 hierarchy between humans and macaque monkeys (12–14). Previously, we observed striking similarities in invariant  
68 visual object recognition behavior between these two primate species, even when measured at very high behavioral  
69 resolution (15, 16). Recent work suggests that non-human primates may also mimic some aspects of human  
70 orthographic processing behavior (17, 18). In particular, Grainger and colleagues showed that baboons can learn  
71 to accurately discriminate visually-presented four-letter English words from pseudo-word strings (17). Crucially, the  
72 authors showed that baboons were not simply memorizing every stimulus, but instead had learned to discriminate  
73 between these two categories of visual stimuli based on the general statistical properties of English spelling, as they  
74 generalized to novel stimuli with above-chance performance. Furthermore, the baboons’ patterns of behavioral  
75 performance across non-word stimuli was similar to the corresponding pattern in literate human adults, who make  
76 infrequent but systematic errors on this task. Taken together, those prior results suggest that non-human primate  
77 models, while not capturing the entirety of human reading abilities, may provide a unique opportunity to investigate  
78 the neuronal mechanisms underlying orthographic processing.

79

80 In light of this opportunity, we investigated the existence of potential neural precursors of visual word form  
81 recognition in the ventral visual pathway of untrained macaque monkeys. Prior neurophysiological and  
82 neuropsychological research in macaque monkeys point to a central role of the ventral visual stream in invariant  
83 object recognition (19–21), with neurons in inferior temporal (IT) cortex, the top-most stage of the ventral stream  
84 hierarchy, exhibiting selectivity for complex visual features and remarkable tolerance to changes in viewing conditions  
85 (e.g. position, scale, and pose) (19, 22, 23). It has been suggested that such neural features could have been coopted  
86 and selected by human writing systems throughout the world (5, 6, 24). Here, we reasoned that if orthographic  
87 processing abilities are supported by “recycling” primate IT cortex – either by minimal adaptations to the IT  
88 representation and/or evolutionary addition of new cortical tissue downstream of IT – then this predicts that the initial  
89 state of the IT representation, as measured in naïve macaque monkeys, should readily serve as a computational  
90 precursor of orthographic processing tests. Investigating, for the first time, the representation of letters and letter  
91 strings in macaque IT cortex would not only directly test this prediction but could also provide initial insights into the  
92 representation of letters and letter strings prior to reading acquisition.

93  
94 To quantitatively test this prediction of the “IT precursor” hypothesis, we first operationally defined a set of  
95 thirty orthographic identification and categorization tasks, such as identifying the presence of a specific letter or  
96 specific bigram within a letter string (invariant letter/bigram identification), or sorting out English words from pseudo-  
97 words (lexical decision). We do not claim this to be an exhaustive characterization of orthographic processing, but  
98 an unbiased starting point for that greater goal. As schematically illustrated in Figure 1A, we then recorded the  
99 spiking activity of hundreds of neural sites in V4 and IT of rhesus macaque monkeys while they passively viewed  
100 images of letters, English words and non-word strings. We then formally tested this prediction of the IT precursor  
101 hypothesis by asking whether adding a simple neural readout machinery on top of the macaque IT representation  
102 could produce a neural substrate of orthographic processing, using biologically plausible linear decoders that perform  
103 those behavioral tasks from the firing responses of those neuronal populations. We found that linear decoders that  
104 learn from the population spiking output of IT cortex easily achieved baboon-level performance on these tasks, and  
105 that the pattern of behavioral performance predicted by this hypothesis was highly correlated with the corresponding  
106 baboon behavioral pattern. These behavioral tests were also met by leading artificial neural network models of the  
107 non-human primate ventral stream, but not by low-level representations of those models. Taken together, these  
108 results show that, even in untrained non-human primates, the population of IT neurons contains an explicit (i.e.  
109 linearly separable), if still imperfect, representation of written words that might have been later “recycled” to support  
110 orthographic processing behaviors in higher primates such as humans.

111

## 112 **Results**

113

114 Our primary goal was to experimentally test the capacity of neural representations in the primate ventral  
115 visual pathway to support orthographic classification tasks. To do so, we recorded the activity of hundreds of neurons  
116 from the top two levels of the ventral visual cortical hierarchy of rhesus macaque monkeys. Neurophysiological

117 recordings were made in four Rhesus monkeys using chronically implanted intracortical microelectrode arrays (Utah)  
118 implanted in the inferior temporal (IT) cortex, the top-most stage of the macaque ventral visual stream hierarchy (IT).  
119 As a control, we also collected data from upstream visual cortical area V4, which provides the dominant input to IT  
120 (Figure 1A). Neuronal responses were measured while each monkey passively viewed streams of images, consisting  
121 of alphabet letters, English words, and pseudo-word strings, presented in a rapid serial visual presentation (RSVP)  
122 protocol at the center of gaze (Fig. 1). Images were presented in randomized order, and each image was shown at  
123 least 25 times. Crucially, monkeys had no previous supervised experience with orthographic stimuli, and they were  
124 not rewarded contingently on the stimuli, but solely for accurately fixating. This experimental procedure resulted in a  
125 large dataset of 510 IT neural sites (and 277 V4 neural sites) in response to up to 1120 images of orthographic  
126 stimuli. To test the sufficiency of the IT representation for orthographic processing, we used simple linear decoders  
127 (as biologically plausible approximations of downstream neural computations, see Methods) to test each neuronal  
128 population on a battery of 30 visual orthographic processing tasks: 20 invariant letter identification tasks, 8 invariant  
129 bigram identification tasks, and two variants of the lexical decision task. For each behavioral test, we used a linear  
130 decoder, which computes a simple weighted sum over the IT population activity, to discriminate between two classes  
131 of stimuli (e.g. words versus pseudo-words). The decoder weights are “learned” using the IT population responses  
132 to a subset of stimuli (using 90% of the stimuli for training), and then the performance of the decoder is tested on  
133 held-out stimuli. The overarching prediction of the “IT precursor” hypothesis was that, if a putative neural mechanism  
134 (i.e. a particular readout of a particular neural population) is sufficient for primate orthographic processing behaviors,  
135 then, it should be easy to learn (i.e. few supervised examples), its learned performance should match the overall  
136 primate performance, and its learned performance should have similar patterns of errors as primates that have  
137 learned those same tasks. This logic has been previously applied to the domain of core object recognition to uncover  
138 specific neural linking hypotheses (25) that have been successfully validated with direct causal perturbation of neural  
139 activity (26, 27).

140

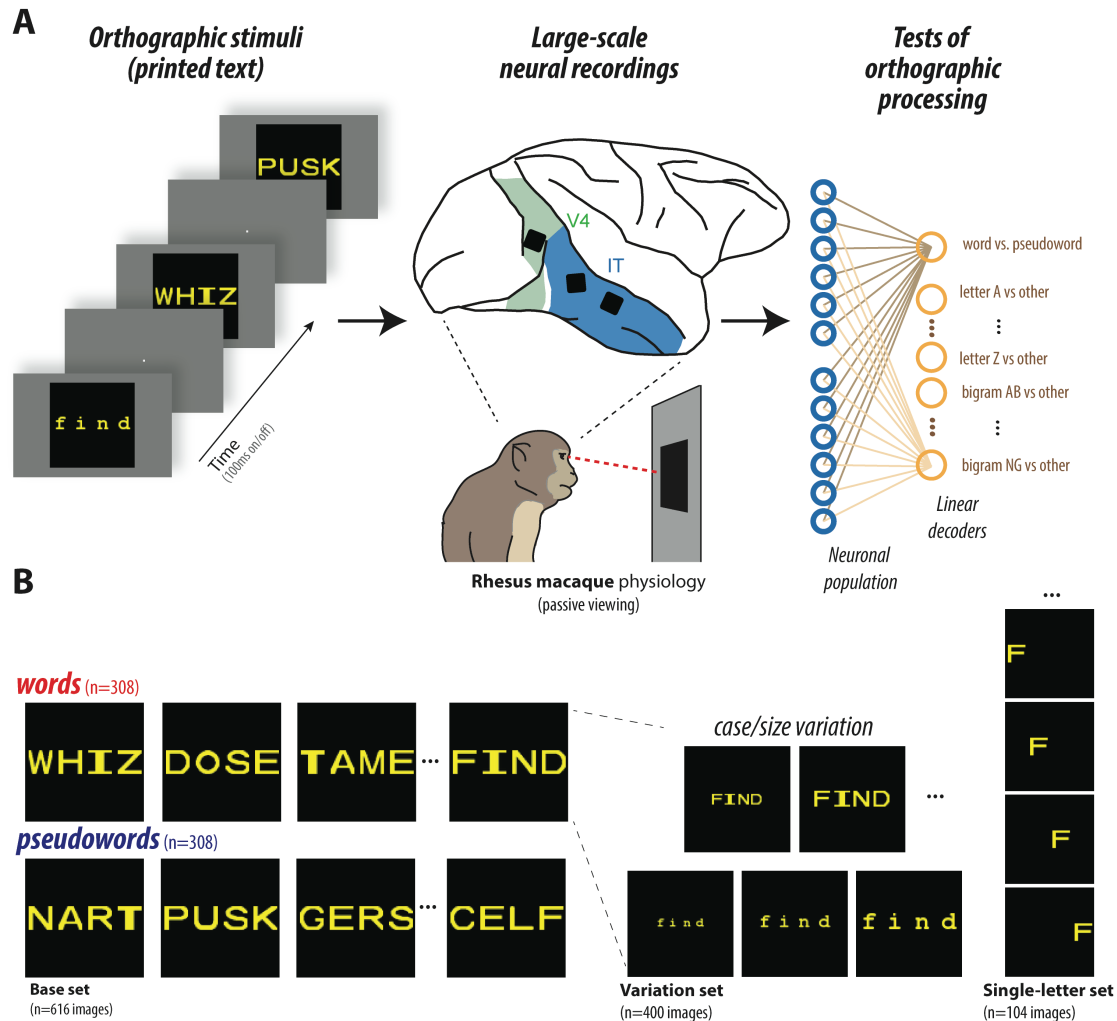


**Figure 1: (A)** Schematic of experiment. We recorded the activity of hundreds of neural sites in IT while monkeys passively fixated images of orthographic stimuli. (As a control, we also recorded from the dominant input to IT, area V4.) We then tested the sufficiency of the IT representation on 30 tests of orthographic processing (e.g. lexical decision, letter identification, etc.) using simple linear decoders. **(B)** Example visual stimuli. Images consisted of four-letter English words and pseudo-word strings presented in canonical views, as well as with variation in case (upper/lower) and size (small/medium/large), and single alphabet letters presented at four different locations.

141

142 **Lexical decision**

143 We first focused on the visual discrimination of English words from pseudo-words (a.k.a. lexical decision)  
 144 using a random subset of the stimuli tested on baboons (17). We collected the response of 510 IT neural sites and  
 145 277 V4 neural sites to a base set of 308 four-letter written words and 308 four-letter pseudo-words (see Figure 1B,  
 146 “base set” for example stimuli). To test the capacity of the IT neural representation to support lexical decision, we  
 147 trained a linear decoder using the IT population responses to a subset of words and pseudo-words, and tested the  
 148 performance of the decoder on held-out stimuli. Note that this task requires generalization of a learned lexical  
 149 classification to novel orthographic stimuli, rather than the mere memorization of orthographic properties. Figure 2A

150 shows the output choices of the linear readout of IT neurons, plotted as the probability of categorizing stimuli as  
 151 words, as compared to behavioral choices of a pool of six baboons, as previously measured by Grainger et al. (17).  
 152 For ease of visualization, the 616 individual stimuli were grouped into equally-sized bins based on the baboon  
 153 performance, separately for words and pseudo-words. We qualitatively observe a tight correspondence between the  
 154 behavioral choices made by baboons and those measured by the linear decoder trained on the IT population. To  
 155 quantify this similarity, we benchmarked both the overall performance (accuracy) and the consistency of pattern of  
 156 errors of the IT population with respect to this previously measured median baboon behavior on the same images.  
 157

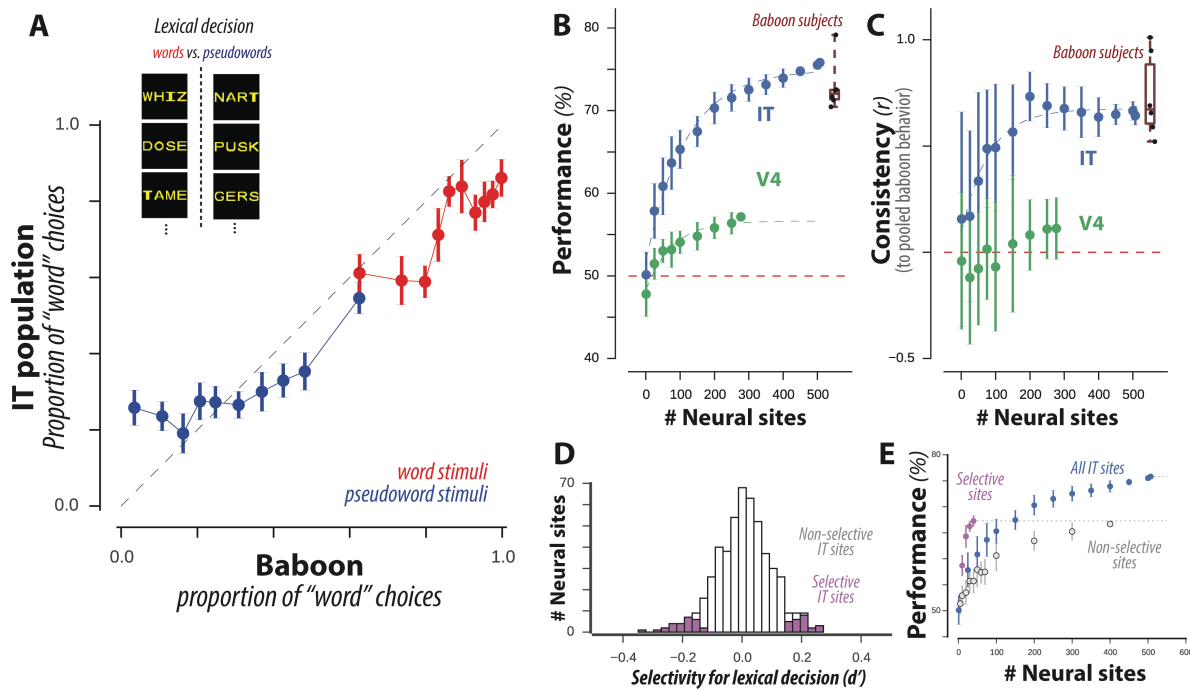


**Figure 2:** (A) Comparison of baboon behavior and a linear readout of IT neurons, plotted as the proportion of stimuli categorized as "words." The 616 individual stimuli were grouped into equally-sized bins based on the baboon performance, separately for words (red) and pseudo-words (blue). Error bars correspond to SEM, obtained via bootstrap resampling over stimuli; dashed line corresponds to unity line, demarking a perfect match between baboon behavior and IT-based decoder outputs. (B) Performance of decoders trained on IT and V4 representations on lexical decision, for varying number of neural sites. Distribution of individual baboon performance is shown on the right. (C) Consistency with baboon behavioral patterns of decoders trained on IT and V4 representations, for varying number of neural sites. (D) Distribution of selectivity of lexical decision for individual IT sites, highlighting the subpopulation of sites with selectivity significantly different from zero. (E) Performance of decoders trained on subpopulation of selective sites from (d) compared to remaining IT sites and all IT sites.

158 We first found that decoders trained on the IT population responses achieved high performance (76% for  
 159 510 neural sites) on lexical decision on new images (Figure 2B). Performance increased steadily with the number of  
 160 neural sites included in the decoder, with about 250 randomly sampled IT neural sites matching the median  
 161 performance of baboons doing this task (Figure 2B, blue). Could any neural population achieve this performance?  
 162 As a first control for this, we tested the upstream cortical area V4. We found that the tested sample of V4 neurons  
 163 did not achieve high performance (only 57% for 277 V4 neural sites), failing to match baboon performance on this  
 164

165 task (Figure 2B, green). Going beyond the summary statistic of average performance, we next tested whether  
166 baboons and neural populations exhibited similar *behavioral patterns* across stimuli, e.g. whether letter strings that  
167 were difficult to categorize for baboons were similarly difficult for these neural populations. To reliably measure  
168 behavioral patterns in each individual baboon subject, we grouped the 616 individual stimuli into equally-sized bins  
169 based on an independent criterion (the average bigram-frequency of each string in English, see Methods),  
170 separately for words and pseudo-words. For both baboons and decoders, we then estimated the average unbiased  
171 performance for each stimulus bin using a sensitivity index ( $d'$ ); this resulted in a ten-dimensional pattern of unbiased  
172 performances. We then measured the similarity between patterns of unbiased performances from a tested neural  
173 population and the pool of baboons using a noise-adjusted correlation (see Methods). We observed that the pattern  
174 of performances obtained from the IT population was highly correlated with the corresponding baboon pool  
175 behavioral pattern (noise-adjusted correlation  $\tilde{\rho} = 0.64$ ; Figure 2C, blue). Perhaps any neural population would  
176 exhibit this baboon-like behavioral pattern? On the contrary, we found that this correlation was significantly higher  
177 than the corresponding value estimated from the V4 population, which is only one visual processing layer away from  
178 IT ( $\tilde{\rho} = 0.11$ ; Figure 2C, green). By holding out data from each baboon subject from the pool, we additionally  
179 estimated the consistency between each individual baboon subject to the remaining pool of baboons (median  $\tilde{\rho} =$   
180  $0.67$ , inter-quartile range =  $0.27$ ,  $n=6$  baboon subjects). This consistency value corresponds to an estimate of the  
181 ceiling of behavioral consistency, accounting for inter-subject variability. Importantly, the consistency of IT-based  
182 decoders is within this baboon behavioral range; this demonstrates that that this neural mechanism is as consistent  
183 to the baboon pool as each individual baboon is to the baboon pool, at this behavioral resolution. Together, these  
184 results suggest that the distributed neural representation in macaque IT cortex is sufficient to explain the lexical  
185 decision behavior of baboons, which itself was previously found to be correlated with human behavior (17).

186  
187 We next explored how the distributed IT population's capacity for supporting lexical decision arose from  
188 single neural sites. Figure 2D shows the distribution of word selectivity of individual sites in units of  $d'$ , with positive  
189 values corresponding to increased firing rate response for words over pseudo-words. We observed that, across the  
190 population, IT did not show strong selectivity for words over pseudo-words (average  $d' = 0.008 \pm 0.09$ , mean, SD  
191 over 510 IT sites), and that no individual IT site was strongly selective for words vs. pseudo-words ( $|d'| < 0.5$  for all  
192 recorded sites). However, a small but significant proportion of sites (10%;  $p < 10^{-5}$ , binomial test with 5% probability of  
193 success) exhibited a weak but significant selectivity for this contrast (inferred by a two-tailed exact test with bootstrap  
194 resampling over stimuli). Note that this subset of neural sites includes both sites that responded preferentially to  
195 words and sites that responded preferentially to pseudo-words. We measured the lexical decision performance of  
196 decoders trained on this subpopulation of neural sites, compared to the remaining subpopulation. Importantly, to  
197 avoid a selection bias in this procedure, we selected and tested neural sites based on independent sets of data  
198 (disjoint split-halves over trial repetitions). As shown in Figure 2E, we observed that decoders trained on this subset  
199 of selective neural sites performed better than a corresponding sample from the remaining non-selective population,  
200 but not as well as decoders trained on the entire population, suggesting that the population's capacity for supporting  
201 lexical decision relies heavily but not exclusively on this small subset of selective neural sites. We next examined



202 whether this subset of selective neural sites was topographically organized on the cortical tissue. For this subset of  
203 neural sites, we did not observe a significant hemispheric bias ( $p=0.13$ , binomial test with probability of success  
204 matching our hemisphere sampling bias), or significant spatial clustering within each  $10 \times 10$  electrode array (Moran's  
205  $I=0.11$ ,  $p=0.70$ , see Methods). Thus, we observed no direct evidence for topographically organized specialization  
206 (e.g. orthographic category-selective domains) in untrained non-human primates, at the resolution of single neural  
207 sites. Taken together, these results suggest that lexical decision behavior could be supported by a sparse, distributed  
208 read-out of the IT representation in untrained monkeys, and provide a baseline against which to compare future  
209 studies of trained monkeys.

210

### 211 **Tests of invariant orthographic processing**

212

213 Importantly, human readers can not only discriminate between different orthographic objects, but also do so  
214 with remarkable tolerance to variability in printed text. For example, readers can effortlessly recognize letters and  
215 words varying in up to two orders of magnitude in size, and are remarkably tolerant to variations in printed font (e.g.  
216 upper vs lower case) (3, 28). To investigate such invariant orthographic processing behaviors, we measured IT  
217 decoder performance for stimuli that vary in font size and font case, for a subsampled set of strings (40 words, 40  
218 pseudo-words, under five different variations for a total of 400 stimuli). To test this, we trained linear decoders on  
219 subsets of stimuli across all variations, and tested on held-out stimuli, for a total of 29 behavioral tests (20 invariant  
220 letter recognition tests, 8 invariant bigram recognition tests, and one test of invariant lexical decision). Figure 3A  
221 shows the performance of a decoder trained on the IT neuronal representation on each of these three types of  
222 behavioral tests, as a function of the neural sample size. For comparison, we also show the same decoder test for  
223 the V4 population. Once again, we observe that the IT population achieved relatively high performance across all  
224 tasks, and that this performance was greater than the corresponding estimated performance from the measured V4  
225 population. We note that performance values for invariant lexical decision should not be directly compared with those  
226 in Figure 2B, as invariant tests here were conducted with fewer training examples for the decoders (i.e. trained/tested  
227 on 40 distinct words/pseudo-words strings, rather than 308 strings in Figure 2B).

228

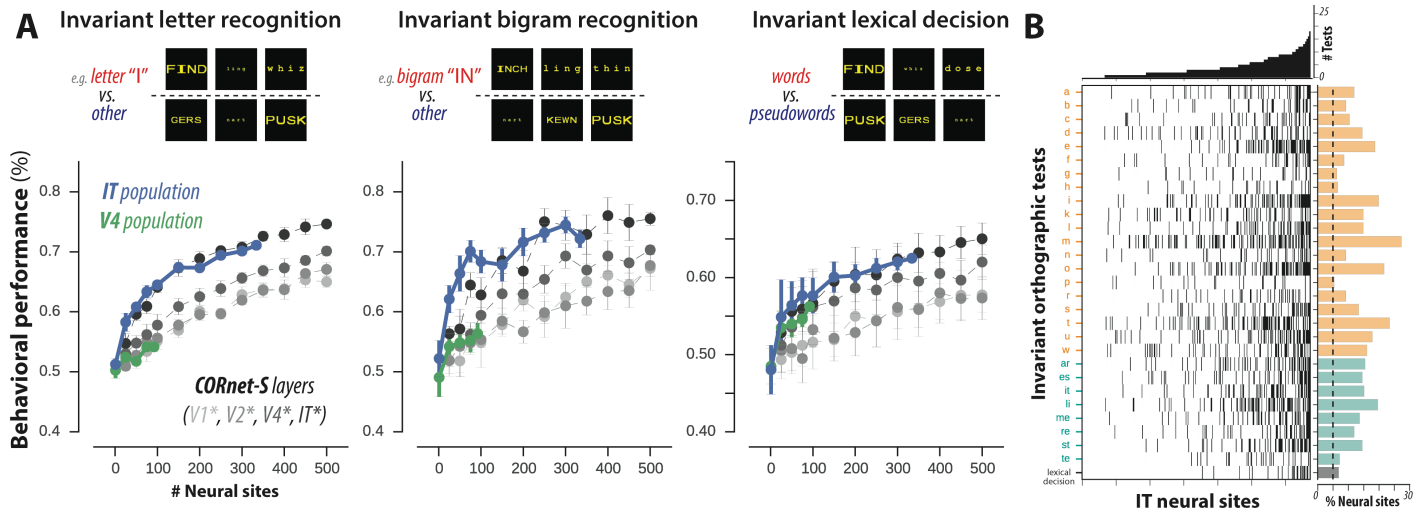


**Figure 3: (A)** Performance of decoders trained on the IT and V4 representations on invariant orthographic tests, grouped into letter identification (n=20 tests), bigram identification (n=8 tests) and invariant lexical decision. Performance of artificial representations sampled from layers of deep convolutional neural network model CORnet-S are shown in grey. **(B)** Selectivity of individual IT sites over 29 invariant orthographic processing tests. The heatmap shows selectivity significantly different from zero over all pairs of neural sites and tests. The histogram above shows the number of behavioral tests ( $N_i$ ) that each neural site exhibited selectivity for; neural sites are ordered by increasing  $N_i$ . The histogram on the right shows the proportion of neural sites exhibiting selectivity for each test; the behavioral tests are ordered alphabetically within each task group (letter identification in orange, bigram identification in cyan, and lexical decision in gray). Dashed line corresponds to proportion of tests expected from chance ( $\alpha = 5\%$ ).

229

230

231

232

233

234

235

236

237

238

239

240

241

242

243

244

245

246

247

We additionally tested the feature representation obtained from a deep recurrent convolutional neural network model of the ventral stream on the exact same behavioral tasks. Specifically, we tested the CORnet-S model (29), as it has recently been shown to best match the computations of the primate ventral visual stream (30, 31) and provides an independently simulated estimate of the neuronal population responses from each retinotopically-defined cortical area in the ventral visual hierarchy (V1, V2, V4, and IT). Figure 3 shows the performance of decoders trained on each simulated neuronal population (gray lines) on invariant letter identification, invariant bigram identification, and invariant lexical decision, as a function of the number of model units used for decoding. We observe that the last layer of CORnet-S (simulated IT) significantly outperforms earlier layers (simulated upstream areas V1, V2, and V4) on these invariant orthographic discrimination tasks, and tightly matches the performance of the actual IT population.

Finally, we tested how the IT population's capacity for these 29 invariant orthographic processing tests was distributed across individual IT neural sites. We computed the selectivity of individual sites in units of  $d'$  for each of these tests, and estimated the statistical significance of each selectivity index using a two-tailed exact test with bootstrap resampling over stimuli (see Methods). Figure 3B shows a heatmap of significant selectivity indices for all pairs of neural sites and behavioral tests; each row corresponds to one behavioral test, each column to a single IT neural site, and filled bins indicate statistically significant selectivity. The histogram above shows the number of behavioral tests that each neural site exhibited selectivity for (median: 3 tests, inter-quartile-range: 5), and the

248 histogram on the right shows the proportion of neural sites exhibiting selectivity for each test (median: 49/337 neural  
249 sites, inter-quartile range: 23/337).

250

251 Taken together, these results suggest that a sparse, distributed read-out of the adult IT representation of  
252 untrained non-human primates is sufficient to support many visual discrimination tasks, including ones in the domain  
253 of orthographic processing, and that that neural mechanism could be learned with a small number of training  
254 examples (median: 48 stimuli; inter-quartile range: 59,  $n = 30$  behavioral tests). Furthermore, this capacity is not  
255 captured by lower-level representations, including neural samples from the dominant visual input to IT (area V4) and  
256 low-level ventral stream representations as approximated by state-of-the-art artificial neural network models of the  
257 ventral stream.

258

### 259 **Encoding of orthographic stimuli**

260

261 Finally, the availability for the first time of IT neuronal responses to orthographic stimuli allowed us to begin  
262 to address the question of how such stimuli are encoded at the single-neuron level. Behavioral and brain-imaging  
263 observations in human readers have led to several proposals concerning the putative neural mechanisms underlying  
264 human orthographic abilities. A presumed front end, common to many models, is a bank of letter detectors (e.g.(2,  
265 32, 33)), i.e. a spatially organized array of input units each sensitive to the presence of a specific letter at a given  
266 location. Additionally, it has been proposed that written words could be encoded by a set of bigram-sensitive units  
267 responding to specific ordered pairs of letters (32). The local combination detector (LCD) hypothesis posits a  
268 hierarchy of cortical representations whereby neurons encode printed words at increasing scale and complexity,  
269 from tuning to simple edges and letters to intermediate combinations of letters (e.g. letter bigrams) and finally to  
270 complex words and morphemes over the cortical hierarchy (2). Other theories have proposed that letter position  
271 information is encoded in the precise timing of spikes (34, 35). To date, it has been difficult to directly test such  
272 hypotheses. Here, to help constrain the space of encoding hypotheses, we characterized the response properties of  
273 hundreds of individual IT neural sites to words and to their component letters.

274

275 We first asked if individual IT neural sites exhibit any selectivity for letters. To test this, we measured the  
276 selectivity of IT responses to each of the 26 alphabet letters, each presented at four different retinal positions. Figure  
277 4A shows the “tuning curve” for three example IT neural sites. Consistent with the known image selectivity and  
278 position tolerance of IT neurons (19, 22, 23), we observed that the responses of these IT neural sites were  
279 significantly modulated by both letter identity and letter position, with each example site responding to some but not  
280 all individual letters. We focused on 222 (out of 338) neural sites with reliable response patterns across the single  
281 letter stimulus set ( $p < 0.01$ , significant Pearson correlation across split-halves over repetitions). The top panel of  
282 Figure 4B shows the average normalized response to each of the 26 letters, across these 222 neural sites. For each  
283 neural site, letters were sorted according to the site’s response magnitude, estimated using half of the data (split-  
284 half of stimulus repetitions) to ensure statistical independence; we then plotted the sorted letter response measured

285 on the remaining half (individual sites in grey, mean  $\pm$  SEM in black). Across the entire population, we observe that  
286 some neural sites reliably respond more to some letters than others, but this modulation is generally not selective  
287 for one or a small number of letters. Rather, sites tended to respond to a broad range of letters, as quantified by the  
288 sparsity of letter responses (Figure 4B, bottom panel). Individual sites were also modulated by letter position (Figure  
289 4C, formatted as in Figure 4B), with a greater response to letters presented contralateral to the recording site, while  
290 also exhibiting substantial tolerance across positions.

291  
292 Next, we asked whether the encoding of letter strings could be approximated as a local combination of  
293 responses to individual letters. To test this, we linearly regressed each site's response to letter strings on the  
294 responses to the corresponding individual letters at the corresponding position, cross-validating over letter strings.  
295 Using the neural responses to all four letters, we observed that the predicted responses of such a linear  
296 reconstruction were modestly correlated with the measured responses to letter strings (see Figure 4D, right-most  
297 bar;  $\tilde{\rho} = 0.29 \pm 0.06$ , median  $\pm$  standard error of median,  $n = 222$  neural sites). To investigate if this explanatory  
298 power arose from all four letters, or whether 4-letter string responses could be explained just as well by a substring  
299 of letters, we trained and tested linear regressions using responses to only some (1, 2, or 3) letters. Given that there  
300 are many possible combinations for each, we selected the best such mapping from the training data, ensuring that  
301 selection and testing were statistically independent. We observed that reconstructions using only some of the letters  
302 were significantly poorer in predicting letter string responses (three letters:  $\tilde{\rho} = 0.12 \pm 0.02$ , median  $\pm$  standard error  
303 of median). Finally, we tested how well a position-agnostic (or "bag of letters") model performed on the same  
304 reconstruction task by trained and test linear regressions that mapped responses of letters, with the incorrect position  
305 (using a fixed, random shuffling of letter positions) on reconstructing the responses to whole letter strings. We found  
306 that this "bag of letters" model performed significantly worse ( $\tilde{\rho} = 0.11 \pm 0.02$ , median  $\pm$  standard error of median).

307  
308 Note that all correlation values reported above were adjusted to account for the reliability of measured neural  
309 responses, such that a fully predictive model would have a noise-adjusted correlation of 1.0 regardless of the finite  
310 amount of data that were collected. Yet, the maximal value of  $\tilde{\rho} = 0.29$  that we obtained using the linear superposition  
311 of position-specific responses to the four letters was substantially lower than 1.0. Thus, the pure summation of neural  
312 responses to individual letter identity and position explained only a small part of the reliable neural responses to 4-  
313 letter strings, suggesting that non-linear responses to local combinations of letters were also present. Future work  
314 using stimuli comprising a larger number of letter combinations can explore to what extent IT neural sites respond,  
315 for instance, to specific letter bigrams, as predicted by some models (2, 32).

316  
317 Taken together, these observations demonstrate that individual IT neural sites in untrained non-human  
318 primates while failing to exhibit strong orthographic specialization, collectively suffice to support a battery of  
319 orthographic tasks. Importantly, these observations establish a number of relevant quantitative baselines, a pre-  
320 registered benchmark to which future studies of the ventral stream representations in monkeys trained on  
321 orthographic discriminations, or in literate humans, could be directly compared to.

322

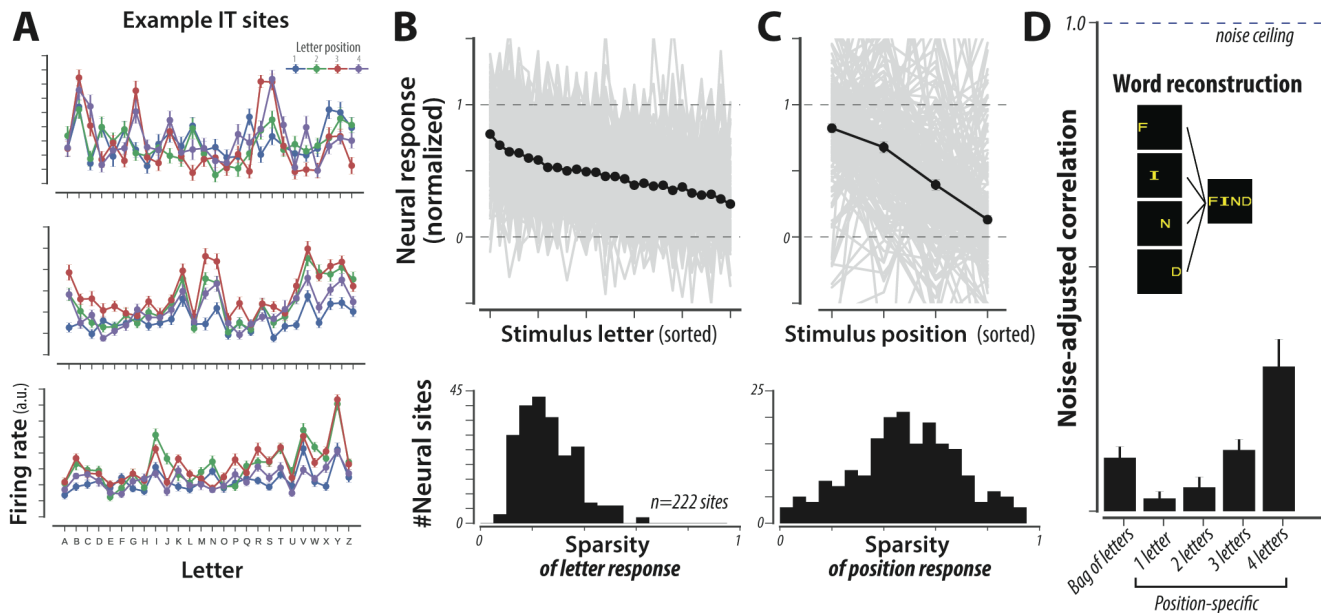


**Figure 4:** (A) Firing rate responses to individual letter stimuli (26 letters at four positions) for three example neurons. (B) (top) Average normalized response to each of the 26 letters, across 222 IT neural sites. For each neural site, letters were sorted according to the site's response magnitude (estimated using an independent half of the data) and plotted in gray. Averaging across the entire population, we observe that neural sites reliably respond more to some letters than others (black, mean  $\pm$  SE across sites; note that SE is very small). However, this modulation is not very selective to individual letters or small numbers of letters, as quantified by the sparsity of letter responses (bottom panel). (C) Individual sites were also modulated by the letter position, exhibiting substantial tolerance across positions (formatted as in B). (D) To test if the encoding of letter strings can be approximated as a local combination of responses to individual letters, we reconstructed letter string responses from letter responses, for each neural site. As illustrated by the inset, we used the neural response to images of individual constituent letters to predict the response to images of the corresponding letter strings; predictions were made using linear regressions, cross-validating over letter strings. The bar plot shows the noise-adjusted correlation of different regression models (median  $\pm$  SE across neural sites). The “bag of letters” model uses responses of each of the four letters, at arbitrary positions, to predict responses of whole letter strings. Each of the position-specific models uses the responses of up to four letters at the appropriate position to predict letter string responses.

323

## 324 Discussion

325

326

327

328

329

330

331

332

A key goal of human cognitive neuroscience is to understand how the human brain supports the ability to learn to recognize written letters and words. This question has been investigated for several decades using human neuroimaging techniques, yielding putative brain regions that may uniquely underlie orthographic abilities (7–9). In the work presented here, we sought to investigate this behavioral domain in the primate ventral visual stream of naïve rhesus macaque monkeys. Non-human primates such as rhesus macaque monkeys have been essential to study the neuronal mechanisms underlying human visual processing, especially in the domain of object recognition where monkeys and humans exhibit remarkably similar behavior and underlying brain mechanisms, both

333 neuroanatomical and functional (13–16, 36, 37). Given this strong homology, and the relative recency of reading  
334 abilities in the human species, we reasoned that the high-level visual representations in the primate ventral visual  
335 stream could serve as a precursor that is recycled by developmental experience for human orthographic processing  
336 abilities. In other words, we hypothesized that the neural representations that directly underlie human orthographic  
337 processing abilities must be strongly constrained by the prior evolution of the primate visual cortex, such that  
338 representations present in naïve, illiterate, non-human primates could be minimally adapted to support orthographic  
339 processing. Here, we observed that orthographic information was explicitly encoded in sampled populations of  
340 spatially distributed IT neurons in naïve, illiterate, non-human primates. Our results are consistent with the hypothesis  
341 that the population of IT neurons in each subject forms an explicit representation of orthographic objects, and could  
342 serve as a common substrate for learning many visual discrimination tasks, including ones in the domain of  
343 orthographic processing.

344

345 We tested a battery of 30 orthographic tests, spanning a lexical decision task (words versus pseudo-words),  
346 invariant letter recognition, and invariant bigram recognition, as well as modifications that required tolerance to  
347 variation in text size and case. We do not claim that these tasks form an exhaustive characterization of orthographic  
348 processing, but rather a good starting point for that greater goal. Importantly, this battery of tasks could not be  
349 accurately performed by linear readout of the predominant input visual representation to IT (area V4) or by  
350 approximations of lower levels of the ventral visual stream, unlike many other coarse discrimination tasks (e.g.  
351 contrasting orthographic and non-orthographic stimuli). We tested arbitrarily sampled IT neural sites, including all  
352 sampled neural sites with significant visual drive. Finally, we modelled plastic changes via a linear classifier, a simple  
353 biologically plausible model of downstream neuronal computations. Indeed, the trained linear decoder performed  
354 binary classifications by computing weighted sums of IT responses followed by a decision boundary, analogous to  
355 synaptic strengths and spiking thresholds of neurons downstream of IT. We note that the successful classifications  
356 we observed do not necessarily imply that the brain exclusively uses IT or the same coding schemes and algorithms  
357 that we have used for decoding. Rather, the existence of this sufficient code in untrained and illiterate non-human  
358 primates suggests that the primate ventral visual stream could be minimally adapted through experience-dependent  
359 plasticity to support orthographic processing behaviors.

360

361 These results are consistent with a variant of the “neuronal recycling” theory, which posits that the features  
362 that support visual object recognition may have been coopted for written word recognition (5, 6, 24). Specifically, this  
363 variant of the theory is that humans have inherited a pre-existing brain system (here, the ventral visual stream) from  
364 recent evolutionary ancestors, and they either inherited or evolved learning mechanisms that enable individuals to  
365 adapt the outputs of that system during their lifespan for word recognition and other core aspects of orthographic  
366 processing. According to this view, pre-reading children already possesses many neurons sensitive to letter-like  
367 shapes such as T, L, +, etc. that – with supervised learning – can be simply combined to support invariant word  
368 recognition. While we observed only weak single IT neuron tuning for individual letters, we note that such visual  
369 encoding is theoretically not the only way that populations of neurons might act as precursors of invariant word

370 recognition behavior, and our IT decoding results empirically demonstrate that here. Regardless of these encoding  
371 alternatives, these results suggest that pre-reading children likely have a neural population representation that can  
372 readily be re-used to learn invariant word recognition. Relatedly, it has been previously proposed that the initial  
373 properties of this system may explain the child's early competence and errors in letter recognition, e.g. explaining  
374 why children tend to make left-right inversion errors by the fact that IT neurons tend to respond invariantly to mirror  
375 images of objects (38–40). Over the course of reading acquisition, this neural representation would become  
376 progressively shaped to support written word recognition in a specific script. The theory may also explain why all  
377 human writing systems throughout the world rely on a universal repertoire of basic shapes (24). As shown in the  
378 present work, those visual features are already well encoded in the ventral visual pathway of illiterate primates, and  
379 may bias cultural evolution by determining which scripts are more easily recognizable and learnable.

380  
381 In addition to testing a prediction of this neuronal recycling hypothesis, we also explored the question of how  
382 orthographic stimuli are encoded in IT neurons. Decades of research has shown that IT neurons exhibit selectivity  
383 for complex visual features with remarkable tolerance to changes in viewing conditions (e.g. position, scale, and  
384 pose) (19, 22, 23). More recent work demonstrates that the encoding properties of IT neurons, in both humans and  
385 monkeys, is best explained by the distributed complex invariant visual features of hierarchical convolutional neural  
386 network models (30, 41, 42). Consistent with this prior work, we here found that the firing rate responses of individual  
387 neural sites in macaque IT was modulated by, but did not exhibit strong selectivity to orthographic properties such  
388 as letters and letter positions. In other words, we did not observe precise tuning as postulated by "letter detector"  
389 neurons, but instead coarse tuning for both letter identity and position. It is possible that, over the course of learning  
390 to read, experience-dependent plasticity could fine-tune the representation of IT to reflect the statistics of printed  
391 words (e.g. single neuron tuning for individual letters or bigrams). Moreover, such experience could alter the  
392 topographic organization to exhibit millimeter-scale spatial clusters that preferentially respond to orthographic stimuli,  
393 as have been shown in juvenile animals in the context of symbol and face recognition behaviors (18, 43). Together,  
394 such putative representational and topographic changes could induce a reorientation of cortical maps towards letters  
395 at the expense of other visual object categories, eventually resulting in the specialization observed in the human  
396 visual word form area (VWFA). However, our results demonstrate that, even prior to such putative changes, the initial  
397 state of IT in untrained monkeys has the capacity to support many learned orthographic discriminations.

398  
399 In summary, we found that the neural population representation in IT cortex in untrained macaque monkeys  
400 is largely capable, with some supervised instruction, to extract explicit representations of written letters and words.  
401 We note that this did not have to be so. Indeed, according to constructivist theories of learning (44), experience  
402 determines cortical organization, and thus the visual representations that underlie orthographic processing should  
403 be largely determined over developmental time-scales by the experience of learning to read. As such, the IT  
404 representation measured in untrained monkeys (or even in illiterate humans) would likely not exhibit the ability to act  
405 as a precursor of orthographic processing. Likewise, orthographic processing abilities could have been critically  
406 dependent on other brain regions, such as speech and linguistic representations, or putative flexible domain-general

407 learning systems, that evolved well after the evolutionary divergence of humans and Old-World monkeys. Instead,  
408 we here report evidence for a “precursor” of visual word form recognition in untrained monkeys. This finding fits with  
409 nativist views of cognitive development, according to which learning rests on pre-existing neural representations  
410 which it only partially reshapes.



## 411 **Methods**

412

413 **Subjects.** The non-human subjects in our experiments were four adult male rhesus macaque monkeys (*Macaca*  
414 *mulatta*, subjects N, B, S, M). Surgical procedures, behavioral training, and neural data collection are described in  
415 detail below. All procedures were performed in compliance with the guideline of National Institutes of Health and the  
416 American Physiological Society, and approved by the MIT Committee on Animal Care.

417

418 **Visual Images.** We randomly subsampled 616 strings (308 words, 308 pseudo-words) from the stimulus set used  
419 to test orthographic processing abilities in baboons by Grainger et al. Word strings consisted of four-letter English  
420 words, whereas pseudo-word strings consisted of nonsense combinations of four letters, with one vowel and three  
421 consonant letters. The entire set of pseudo-words contained bigrams that ranged from those that are very common  
422 in the English language (e.g. "TH") to those that are very uncommon (e.g. "FQ"), as quantified by a broad distribution  
423 of English bigram frequency (median = 95, inter-quartile range = 1366; in units of count per million). As such, given  
424 the previously established link between bigram frequency and difficulty in lexical decision (17), orthographic stimuli  
425 spanned a range of difficulties for the word vs pseudo-word lexical decision task. From these 616 strings, we then  
426 generated images of these strings under different variations generative parameters in font size (small/medium/large  
427 size) and font case (upper/lower case), fixing the font type (monotype), color (yellow), thus creating a total of 3696  
428 images. We additionally generated images of individual alphabet letters at each of the possibly locations (26 letters  
429 x 4 locations x 6 variations in font case/size). We measured IT and V4 responses from passively fixating rhesus  
430 macaque monkeys (see below) for a subset of 1120 images from this stimulus set, and used previously measured  
431 behavior from trained baboons from the study by Grainger and colleagues (17). Visual images were presented to  
432 span 8° of visual angle, with each individual letter of size 0.8°, 1.2, and 1.6° for small, medium, and large variations.  
433

434

435 **Baboon behavior.** Baboon behavioral data from six guinea baboons performing a lexical decision task was obtained  
436 from prior work (17). We focused our analysis on the aforementioned subsampled stimulus set (616 strings).

437

### 438 **Large scale multielectrode recordings.**

439

440 ***Surgical implant of chronic micro-electrode arrays.*** We surgically implanted each monkey with a head post under  
441 aseptic conditions. After behavioral training, we implanted multiple 10 × 10 micro-electrode arrays (Utah arrays;  
442 Blackrock Microsystems) in V4 and IT cortex of each monkey. A total of 96 electrodes were connected per array.  
443 Each electrode was 1.5 mm long and the distance between adjacent electrodes was 400 μm. Array placements were  
444 guided by the sulcus pattern, which was visible during surgery. The electrodes were accessed through a  
445 percutaneous connector that allowed simultaneous recording from all 96 electrodes from each array. All behavioral  
446 training and testing were performed using standard operant conditioning (fluid reward), head stabilization, and real-  
447 time video eye tracking.

448 **Eye Tracking.** We monitored eye movements using video eye tracking (SR Research EyeLink 1000). Using operant  
449 conditioning and water reward, our two subjects were trained to fixate a central white square ( $0.2^\circ$ ) within a square  
450 fixation window that ranged from  $\pm 2^\circ$ . At the start of each behavioral session, monkeys performed an eye-tracking  
451 calibration task by making a saccade to a range of spatial targets and maintaining fixation for 500 ms. Calibration  
452 was repeated if drift was noticed over the course of the session.

453  
454 **Electrophysiological Recording.** During each recording session, band-pass filtered (0.1 Hz to 10 kHz) neural  
455 activity was recorded continuously at a sampling rate of 20 kHz using Intan Recording Controller (Intan Technologies,  
456 LLC). The majority of the data presented here were based on multiunit activity, hence we refer to “neural sites.” We  
457 detected the multiunit spikes after the raw data was collected. A multiunit spike event was defined as the threshold  
458 crossing when voltage (falling edge) deviated by less than three times the standard deviation of the raw voltage  
459 values. In this manner, we collected neural data from macaque V4 and IT from four male adult monkeys (N, B, S, M,  
460 weights in kg) in a piecewise manner. We focused our analyses on neural sites that exhibited significant visual drive  
461 (determined by  $p < 0.001$  comparing baseline activity to visually driven activity); this resulted in 510 IT neural sites  
462 and 277 V4 neural sites. Our array placements allowed us to sample neural sites from different parts of IT, along the  
463 posterior to anterior axis. However, we did not consider the specific spatial location of the site, and treated each site  
464 as a random sample from a pooled IT population. For each neural site, we estimated the repetition-averaged firing  
465 rate response in two temporal windows (70ms-170ms and 170ms-270ms after stimulus onset) and concatenated  
466 these firing rates for decoding analyses. Single unit analyses focused on the 70ms-170ms time interval.

#### 467 **Tests of orthographic processing**

468  
469  
470 **Linear decoders.** To test the capacity of ventral stream neural representations to support orthographic processing  
471 tasks, we used linear decoders to discriminate between two classes of stimuli (e.g. words versus pseudo-words)  
472 using the firing rate responses of neural populations. We used binary logistic regression classifiers with ten-fold  
473 cross-validation: decoder weights were learned using the neural population responses to 90% of stimuli and then  
474 the performance of the decoder is tested on held-out 10% of stimuli, repeating 10 times to test each stimulus. We  
475 repeated this process 10 times with random sampling of neurons. This procedure produces an output class  
476 probability for each tested stimulus, and we took the maximum of those as the behavioral “choice” of the decoded  
477 neural population.

478  
479 **Deep neural network model behavior.** We additionally tested a deep neural network model of the primate ventral  
480 stream on the exact same images and tasks. We used CORnet-S, a deep recurrent convolutional neural network  
481 model that has recently been shown to best match the computations of the primate ventral visual stream (29, 31).  
482 CORnet-S approximates the hierarchical structure of the ventral stream, with four areas each mapped to the four  
483 retinotopically-defined cortical area in the ventral visual hierarchy (V1, V2, V4, and IT). To do so, we first extracted  
484 features from each CORnet-S layer on the same images. As with neural features, we trained back-end binary logistic

485 regression classifiers to determine the ten-fold cross-validated output class probability for each image and for each  
486 label.

487

488 **Behavioral metrics.** For each behavioral test, we measured the average unbiased performance (or balanced  
489 accuracy) as  $acc = \frac{HR + (1 - FAR)}{2}$ , where HR and FAR correspond to the hit-rate and false-alarm-rate across all stimuli.

490 For the lexical decision task, we additionally estimated behavioral patterns across stimuli. To reliably measure  
491 behavioral patterns in each individual baboon subject, we grouped the 616 individual stimuli into ten equally-sized  
492 bins separately for words and pseudo-words; bins were defined based on the average bigram-frequency of each  
493 string in English. We then estimated the average unbiased performance for each stimulus bin using a sensitivity  
494 index:  $d' = Z(HR) - Z(FAR)$  (45), where HR and FAR correspond to the hit-rate and false-alarm-rate across all  
495 stimuli within the bin. Across stimulus bins, this resulted in a ten-dimensional pattern of unbiased performances.

496

497 **Behavioral consistency.** To quantify the behavioral similarity between baboons and candidate visual systems (both  
498 neural and artificial) with respect to the pattern of unbiased performance described above, we used a measure called  
499 “consistency” ( $\tilde{\rho}$ ) as previously defined (46), computed as a noise-adjusted correlation of behavioral signatures (47).

500 For each system, we randomly split all behavioral trials into two equal halves and estimated the pattern of unbiased  
501 performance on each half, resulting in two independent estimates of the system’s behavioral signature. We took the  
502 Pearson correlation between these two estimates of the behavioral signature as a measure of the reliability of that  
503 behavioral signature given the amount of data collected, i.e. the split-half internal reliability. To estimate the  
504 consistency, we computed the Pearson correlation over all the independent estimates of the behavioral signature  
505 from the model ( $\mathbf{m}$ ) and the primate ( $\mathbf{p}$ ), and we then divide that raw Pearson correlation by the geometric mean of  
506 the split-half internal reliability of the same behavioral signature measured for each system:  $\tilde{\rho}(\mathbf{m}, \mathbf{p}) = \frac{\rho(\mathbf{m}, \mathbf{p})}{\sqrt{\rho(\mathbf{m}, \mathbf{m})\rho(\mathbf{p}, \mathbf{p})}}$ .

507 Since all correlations in the numerator and denominator were computed using the same number of trials, we did not  
508 need to make use of any prediction formulas (e.g. extrapolation to larger number of trials using Spearman-Brown  
509 prediction formula). This procedure was repeated 10 times with different random split-halves of trials. Our rationale  
510 for using a reliability-adjusted correlation measure for consistency was to account for variance in the behavioral  
511 signatures that is not replicable by the experimental condition (image and task).

512

513 **Single neuron analyses.** For each neural site, we estimated the selectivity with respect to a number of contrasts  
514 (e.g. word vs pseudo-word) using a sensitivity index:  $d'_{x,y} = \frac{\mu_x - \mu_y}{\sqrt{\frac{1}{2}(\sigma_x^2 + \sigma_y^2)}}$  (45). We obtained uncertainty estimates for

515 single neuron selectivity indices by bootstrap resampling over stimuli, and inferred statistical significance using two-  
516 tailed exact tests on the bootstrapped distributions. We determined whether neural sites that exhibited significant  
517 selectivity for lexical decisions were topographically organized across the cortical tissue using Moran’s  $I$  (48), a metric  
518 of spatial autocorrelation. We compared the empirically measured autocorrelation (averaged over six electrode  
519 arrays) to the corresponding distributions expected by chance, obtained by shuffling each electrode’s selectivity 100  
520 times.

521 **References**

522

- 523 1. Grainger J, Dufau S, Ziegler JC (2016) A Vision of Reading. *Trends in Cognitive Sciences*  
524 20(3):171–179.
- 525 2. Dehaene S, Cohen L, Sigman M, Vinckier F (2005) The neural code for written words: a proposal.  
526 *Trends Cogn Sci* 9(7):335–41.
- 527 3. Legge GE, Bigelow CA (2011) Does print size matter for reading? A review of findings from vision  
528 science and typography. *J Vis* 11(5). doi:10.1167/11.5.8.
- 529 4. Cohen L, et al. (2000) The visual word form area: Spatial and temporal characterization of an initial  
530 stage of reading in normal subjects and posterior split-brain patients. *Brain* 123:291–307.
- 531 5. Dehaene S (2009) *Reading in the brain* (Penguin Viking, New York).
- 532 6. Dehaene S, Cohen L (2007) Cultural recycling of cortical maps. *Neuron* 56(2):384–98.
- 533 7. Dehaene-Lambertz G, Monzalvo K, Dehaene S (2018) The emergence of the visual word form:  
534 Longitudinal evolution of category-specific ventral visual areas during reading acquisition. *PLoS Biol*  
535 16(3):e2004103.
- 536 8. Dehaene S, et al. (2010) How learning to read changes the cortical networks for vision and  
537 language. *Science* 330(6009):1359–64.
- 538 9. Dehaene S, Cohen L, Morais J, Kolinsky R (2015) Illiterate to literate: behavioural and cerebral  
539 changes induced by reading acquisition. *Nat Rev Neurosci* 16(4):234–244.
- 540 10. Felleman DJ, Van Essen DC (1991) Distributed hierarchical processing in the primate cerebral  
541 cortex. *Cereb Cortex* 1(1):1–47.
- 542 11. Passingham R (2009) How good is the macaque monkey model of the human brain? *Current*  
543 *opinion in neurobiology* 19:6–11.
- 544 12. Kriegeskorte N, et al. (2008) Matching categorical object representations in inferior temporal cortex  
545 of man and monkey. *Neuron* 60:1126–1141.
- 546 13. Mantini D, et al. (2012) Interspecies activity correlations reveal functional correspondence between  
547 monkey and human brain areas. *Nature methods* 9:277–282.
- 548 14. Orban GA, Van Essen D, Vanduffel W (2004) Comparative mapping of higher visual areas in  
549 monkeys and humans. *Trends in cognitive sciences* 8:315–324.
- 550 15. Rajalingham R, Schmidt K, DiCarlo JJ (2015) Comparison of Object Recognition Behavior in  
551 Human and Monkey. *The Journal of Neuroscience* 35(35):12127–12136.
- 552 16. Rajalingham R, et al. (2018) Large-scale, high-resolution comparison of the core visual object  
553 recognition behavior of humans, monkeys, and state-of-the-art deep artificial neural networks.  
554 *Journal of Neuroscience* 38(33):7255–7269.

- 555 17. Grainger J, Dufau S, Montant M, Ziegler JC, Fagot J (2012) Orthographic processing in baboons  
556 (Papio papio). *Science* 336(6078):245–248.
- 557 18. Srihasam K, Vincent JL, Livingstone MS (2014) Novel domain formation reveals proto-architecture  
558 in inferotemporal cortex. *Nat Neurosci* 17(12):1776–1783.
- 559 19. Tanaka K (1996) Inferotemporal cortex and object vision. *Annual Review of Neuroscience* 19:109–  
560 139.
- 561 20. Logothetis NK, Sheinberg DL (1996) Visual object recognition. *Annual review of neuroscience*  
562 19(1):577–621.
- 563 21. DiCarlo JJ, Zoccolan D, Rust NC (2012) How does the brain solve visual object recognition?  
564 *Neuron* 73:415–434.
- 565 22. Logothetis NK, Pauls J, Poggio T (1995) Shape representation in the inferior temporal cortex of  
566 monkeys. *Current Biology* 5(5):552–563.
- 567 23. Rust NC, DiCarlo JJ (2010) Selectivity and tolerance (“invariance”) both increase as visual  
568 information propagates from cortical area V4 to IT. *The Journal of Neuroscience* 30:12978–12995.
- 569 24. Changizi MA, Zhang Q, Ye H, Shimojo S (2006) The Structures of Letters and Symbols throughout  
570 Human History Are Selected to Match Those Found in Objects in Natural Scenes. *Am Nat*  
571 167(5):E117-39.
- 572 25. Majaj NJ, Hong H, Solomon EA, DiCarlo JJ (2015) Simple Learned Weighted Sums of Inferior  
573 Temporal Neuronal Firing Rates Accurately Predict Human Core Object Recognition Performance.  
574 *The Journal of Neuroscience* 35:13402–13418.
- 575 26. Rajalingham R, DiCarlo JJ (2019) Reversible inactivation of different millimeter-scale regions of  
576 primate IT results in different patterns of core object recognition deficits. *Neuron*.
- 577 27. Afraz A, Boyden ES, DiCarlo JJ (2015) Optogenetic and pharmacological suppression of spatial  
578 clusters of face neurons reveal their causal role in face gender discrimination. *Proceedings of the*  
579 *National Academy of Sciences* 112(21):6730–6735.
- 580 28. Dehaene S, et al. (2001) Cerebral mechanisms of word masking and unconscious repetition  
581 priming. *Nat Neurosci* 4(7):752–8.
- 582 29. Kubilius J, et al. (2018) CORnet: modeling the neural mechanisms of core object recognition.  
583 *BioRxiv*:408385.
- 584 30. Schrimpf M, et al. (2018) Brain-Score: which artificial neural network for object recognition is most  
585 brain-like? *BioRxiv*:407007.
- 586 31. Kar K, Kubilius J, Schmidt K, Issa EB, DiCarlo JJ (2019) Evidence that recurrent circuits are critical  
587 to the ventral stream’s execution of core object recognition behavior. *Nature neuroscience*  
588 22(6):974.
- 589 32. Grainger J, van Heuven W (2003) Modeling Letter Position Coding in Printed Word Perception. *The*  
590 *Mental Lexicon*, ed Bonin P (Nova Science Publishers, New York), pp 1–24.

- 591 33. McClelland JL, Rumelhart DE (1981) An interactive activation model of context effects in letter  
592 perception: I. An account of basic findings. *Psychological review* 88(5):375.
- 593 34. Whitney C (2001) How the brain encodes the order of letters in a printed word: the SERIOL model  
594 and selective literature review. *Psychon Bull Rev* 8(2):221–43.
- 595 35. Davis CJ (2010) The spatial coding model of visual word identification. *Psychol Rev* 117(3):713–58.
- 596 36. Miranda-Dominguez O, et al. (2014) Bridging the gap between the human and macaque  
597 connectome: a quantitative comparison of global interspecies structure-function relationships and  
598 network topology. *The Journal of Neuroscience* 34:5552–5563.
- 599 37. Tootell RB, Tsao D, Vanduffel W (2003) Neuroimaging weighs in: humans meet macaques in  
600 “primate” visual cortex. *The Journal of Neuroscience* 23:3981–3989.
- 601 38. Rollenhagen JE, Olson CR (2000) Mirror-image confusion in single neurons of the macaque  
602 inferotemporal cortex. *Science* 287(5457):1506–8.
- 603 39. Freiwald WA, Tsao DY (2010) Functional compartmentalization and viewpoint generalization within  
604 the macaque face-processing system. *Science* 330(6005):845–51.
- 605 40. Dehaene S, et al. (2010) Why do children make mirror errors in reading? Neural correlates of mirror  
606 invariance in the visual word form area. *NeuroImage* 49(2):1837–48.
- 607 41. Yamins DL, et al. (2014) Performance-optimized hierarchical models predict neural responses in  
608 higher visual cortex. *Proceedings of the National Academy of Sciences*:201403112.
- 609 42. Khaligh-Razavi S-M, Kriegeskorte N (2014) Deep supervised, but not unsupervised, models may  
610 explain IT cortical representation. *PLoS computational biology* 10:e1003915.
- 611 43. Srihasam K, Mandeville JB, Morocz IA, Sullivan KJ, Livingstone MS (2012) Behavioral and  
612 Anatomical Consequences of Early versus Late Symbol Training in Macaques. *Neuron* 73(3):608–  
613 619.
- 614 44. Quartz SR, Sejnowski TJ (1997) The neural basis of cognitive development: A constructivist  
615 manifesto. *Behavioral and brain sciences* 20(4):537–556.
- 616 45. Macmillan NA (1993) Signal detection theory as data analysis method and psychological decision  
617 model.
- 618 46. Johnson KO, Hsiao SS, Yoshioka T (2002) Neural coding and the basic law of psychophysics. *The  
619 Neuroscientist* 8(2):111–121.
- 620 47. DiCarlo JJ, Johnson KO (1999) Velocity invariance of receptive field structure in somatosensory  
621 cortical area 3b of the alert monkey. *Journal of Neuroscience* 19(1):401–419.
- 622 48. Moran PA (1950) Notes on continuous stochastic phenomena. *Biometrika* 37(1/2):17–23.
- 623